



HAL
open science

Impact of Residual Stresses on the Fatigue Behavior of a Nickel-Based Superalloy

Amélie Morançais, Mathieu Fèvre, Pascale Kanoute, Serge Kruch, Manuel François

► To cite this version:

Amélie Morançais, Mathieu Fèvre, Pascale Kanoute, Serge Kruch, Manuel François. Impact of Residual Stresses on the Fatigue Behavior of a Nickel-Based Superalloy. *Materials Science Forum*, 2013, 768-769, pp.747-754. 10.4028/www.scientific.net/MSF.768-769.747 . hal-02278279

HAL Id: hal-02278279

<https://utt.hal.science/hal-02278279>

Submitted on 28 Aug 2023

HAL is a multi-disciplinary open access archive for the deposit and dissemination of scientific research documents, whether they are published or not. The documents may come from teaching and research institutions in France or abroad, or from public or private research centers.

L'archive ouverte pluridisciplinaire **HAL**, est destinée au dépôt et à la diffusion de documents scientifiques de niveau recherche, publiés ou non, émanant des établissements d'enseignement et de recherche français ou étrangers, des laboratoires publics ou privés.

Impact of residual stresses on the fatigue behavior of a Nickel-based superalloy

A. Morançais^{1,a}, M. Fèvre^{1&2,a}, P. Kanoute^{1&3,c}, S. Kruch^{1,d} and M. François^{3,e}

¹ONERA – The French Aerospace Lab, F-92322 Châtillon, France

²LEM UMR 104 CNRS-ONERA, F-92322 Châtillon, France

³ICD-LASMIS, UMR CNRS 6279 Université de Technologie de Troyes, rue Marie Curie 10004 TROYES CEDEX, France

^aamelie.morancais@onera.fr, ^bmathieu.fevre@onera.fr, ^cpascale.kanoute@onera.fr,
^dserge.kruch@onera.fr, ^emanuel.francois@utt.fr

Keywords: residual stresses, stress relaxation, viscoplasticity, cyclic loading, fatigue.

Abstract. The fatigue life of aircraft turbine engine discs depends on the mechanical stress state and the microstructure of the constituting alloy. The residual stresses (RS) induced by machining operations and heat treatments is one of the controlling parameters; however, they are likely to evolve during the service life. The present paper presents a method which takes into account RS and their relaxation in fatigue life calculation. This method is applied to a representative specimen made of N18 nickel based polycrystalline superalloy. RS level is first measured using X-ray diffraction on shot-peened specimen. It is then introduced in a Finite Element Model (FEM) which uses a multiaxial extension of the Smith-Watson-Topper model. It was found that compressive residual stresses introduced by a shot-peening treatment have almost no influence for high cyclic strain levels but improve the fatigue life for lower levels.

Introduction

Nickel based superalloys are used in turbine engine applications because of their mechanical properties at high temperatures, their ability to endure aggressive environments (oxidation, corrosion) and their tolerance to damage. During the engine service, High Pressure turbine discs are exposed to thermomechanical loadings at temperatures up to 700°C. One of the failure mechanisms is associated with crack nucleation and growth from the surface of the component. The life time of the High-Pressure turbine discs strongly depends on both the microstructure of the alloy and its mechanical stress state. Indeed, nucleation sites can be grain facets and/or ceramic inclusions arising from the production of metallic powders. For fine grain materials, which have the longest fatigue life, both types of nucleation sites are involved, causing a strong dispersion in fatigue test results. For large grain materials, nucleation sites are mainly grain facets and the dispersion is smaller but the fatigue life is generally lower [1]. The prediction of the lifetime of the turbine disc, and thus the maintenance intervals, are consequently easier for alloys with large grain sizes. The effects of residual stresses on fatigue life of polycrystalline superalloys have been widely investigated and the capacity of compressive residual stresses to retard crack growth is commonly demonstrated [2-3]. Manufacturing techniques including forging, heat treatments, machining and shot-peening generate residual stresses which evolve during service conditions. As RS are superposed to the applied load, the quantification of their level is crucial to accurately estimate the lifetime of critical components. Life prediction models calibrated on tensile, creep and cyclic fatigue tests and taking into account the geometry of the component and the loading conditions are developed to design discs and define thermal and mechanical treatments resulting in higher performances [1]. The incorporation of residual stresses into the modeling is thus essential for the development of safer critical components [4].

The aim of the present paper is to take into account the effects of residual stresses in the fatigue life assessment of turbine discs. The method is based on the use of Chaboche type constitutive behavior with multi-kinematic hardening with threshold effects to obtain the evolution of the mechanical stress and strain states under cyclic loading. Once the stabilized state is reached, a Smith-Watson-Topper scheme is used to calculate the number of cycles to crack initiation.

Experiments

Investigated specimens. Measurements are performed on a flat specimen (Figure 1) manufactured from a N18 nickel based alloy. The chemical composition is given in Table 1. The cast and forged material was treated by:

- a solution heat treatment above the γ' solvus and air quenched
- a two-steps aging treatment.

The obtained microstructure exhibits cubical γ' precipitates of composition Ni_3Al with the L1_2 structure embedded in a γ matrix with the A_1 structure. The microstructure analysis using optical microscopy (Figure 1) reveals an average grain size of $50\mu\text{m}$.

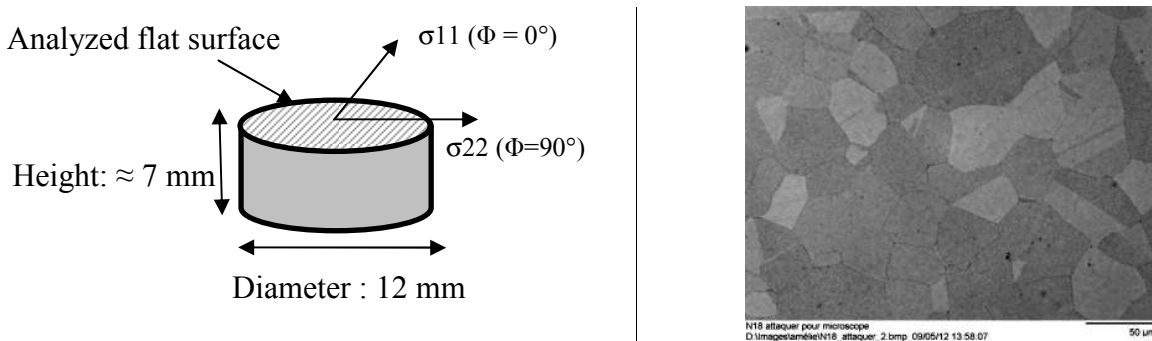


Figure 1: Left: Specimen geometry – Right: Microstructure on surface (grain size $\sim 50\mu\text{m}$).

Table 1: Composition of the Ni-based superalloy material N18 (wt%).

Components	Ni	Cr	Mo	Al	Co	Ti	Hf	Zr	Ta	C	B	Fe
N18 (%)	57.05	11.5	6.47	4.41	15.6	4.37	0.52	0.03	0.016	0.016	0.016	0.11

The specimen is then prepared as follow: Turning, Grinding, mechanical Polishing (TGmP) and shot-peening (F15A Almen intensity).

Residual Stress measurements. The residual stress state due to specimen preparation was determined by X-ray diffraction with the classical $\sin^2\Psi$ method on a 4-circles diffractometer equipped with a rotating copper anode and a scintillation counter [5 - 6]. Measurement conditions are summarized in Table 2. The irradiated area is about 1.4 mm^2 and the average penetration depth is about $12\mu\text{m}$. $\Phi=0^\circ$ corresponds to a direction perpendicular to the polishing grooves of the specimen.

As the lattice parameters of γ and γ' phases are very close (smaller than 0.2%) the diffraction peaks contain the contribution of both phases. They were treated globally by a pseudo-Voigt function to obtain the elastic strain for each Ψ inclination.

Table 2: Summary of the measurement conditions.

Method used	$\sin^2 \Psi$ method – χ mode
Diffraction plane	{024} (146°) and {133}(138°), Cu K α 1+K α 2 ($\lambda = 1.540562 \text{ \AA}$)
2 θ	From 130° to 155° / 0.16° steps (time : 90sec/point), oscillation
Number of tilt Ψ	13 between -60° and 65°
Φ angles	0° and 90°
X-ray elasticity constants [5]	$S_1(133) = -1.17 \times 10^{-6} \text{ MPa}^{-1}$ and $\frac{1}{2} S_2(133) = 5.68 \times 10^{-6} \text{ MPa}^{-1}$ $S_1(024) = -1.48 \times 10^{-6} \text{ MPa}^{-1}$ and $\frac{1}{2} S_2(024) = 6.61 \times 10^{-6} \text{ MPa}^{-1}$

The σ_{11} and σ_{22} depth profiles are presented on Figure 2. The profile is typical of shot-peened specimens with a maximum of -900 MPa reached at 55 μm below the surface [7]. The uncertainty which is close to 30 MPa near the surface increases as a function of depth and is close to 90 MPa at 76 μm . Because of grain size issues (grain size after heat-treatment is around 50 μm), the values beyond 80 μm were considered as not reliable and were omitted. To introduce the stress profile in the Finite Element Model, it was assumed that the layer in compression is about 100 μm and the profile was completed arbitrarily.

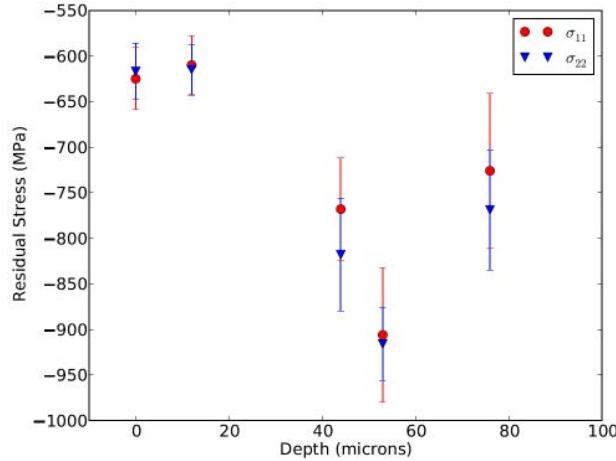


Figure 2: Residual stress profiles after machining and shot-peening.

Fatigue life analysis

The aim of the Finite Element analysis is to introduce the residual stress profile at the beginning of the calculations and to study their possible relaxation as well as the evolution of hardening variables using the finite element Z-set/Zebulon code.

Constitutive equations. The N18 superalloy has been characterized and identified at 450°C in a previous study by Boittin [1].

The elasto-viscoplastic behavior is characterized by a non-linear isotropic hardening, four non-linear kinematics hardening with thresholds and one linear kinematic hardening. The complexity of such constitutive equations to describe the non-linear behavior is justified by the need to deliver an accurate estimation of the crack initiation in the structure. Indeed, the fatigue lifetime estimation requires a precise evaluation of both the stress and the strain states at each integration point of the structure at the stabilized cycle. A major key point is to correctly reproduce the cyclic hardening and the limited mean stress relaxation for cyclic loads performed in a given range of strain amplitudes. Indeed, it has been experimentally highlighted for strain controlled cyclic tests (strain

ratio R_e equal to 0) that the mean stress does not relax to 0 for strain amplitudes lower than 1%. The introduction in the modeling of non-linear kinematic hardening with thresholds, as proposed by Chaboche, is one of the best ways to reproduce such experimental observation [8].

The constitutive equations are summarized as follows, based on the classical separation of the total strain ($\underline{\varepsilon}$) in an elastic ($\underline{\varepsilon}_e$) and plastic ($\underline{\varepsilon}_p$) part:

$$\underline{\varepsilon} = \underline{\varepsilon}_e + \underline{\varepsilon}_p = \underline{\underline{C}}^{-1} : \underline{\sigma} + \underline{\varepsilon}_p \quad \text{where } \underline{\underline{C}} \text{ is the elasticity tensor}$$

$$f = J(\underline{\sigma} - \underline{\chi}) - R - R_0 \quad \text{with} \quad J(\underline{\sigma} - \underline{\chi}) = \sqrt{\frac{3}{2}(\underline{\sigma} - \underline{\chi})' : (\underline{\sigma} - \underline{\chi})'}$$

where f is a function reflecting the evolution of the elastic domain, $\underline{\chi}$ and R denote respectively the kinematic and linear hardening, and R_0 the initial yield strength.

The evolution of the plastic deformation is defined as follows:

$$\dot{\underline{\varepsilon}}_p = \frac{3}{2} \left\langle \frac{J(\underline{\sigma}' - \underline{\chi}') - R - R_0}{K} \right\rangle^n \frac{\underline{\sigma}' - \underline{\chi}'}{J(\underline{\sigma}' - \underline{\chi}')} \quad \text{where } \underline{\sigma}' \text{ is the deviatoric part of } \underline{\sigma}.$$

The non linear isotropic hardening is defined by $R = \gamma(1 - e^{-bp})$ where γ and b are material parameters and p denotes the cumulative plastic strain.

Finally, the non linear kinematic hardening with thresholds is written as:

$$\dot{\underline{\chi}}_i = \frac{2}{3} \underline{\underline{C}} \dot{\underline{\alpha}}_i \quad \text{with} \quad \dot{\underline{\alpha}}_i = \dot{p} \left(n - \frac{3}{2} \frac{D_i}{C_i} \Phi_i \underline{\chi}_i \right) \quad \text{and} \quad n = \frac{\partial f}{\partial \underline{\sigma}} = \frac{3(\underline{\sigma} - \underline{\chi})'}{2J(\underline{\sigma} - \underline{\chi})}$$

$$\Phi_i = \left\langle \frac{D_i J(\underline{\chi}) - \omega_i C_i}{1 - \omega_i} \right\rangle^{m_1} \frac{1}{(D_i J(\underline{\chi}))^{m_2}} \underline{I}$$

Sixteen parameters must be identified Q , b , C_i , D_i , ω_i , m_1 and m_2 ($i=1$ to 4)

In order to show the efficiency of the model, Figure 3 presents the stabilized mean-stress as a function of the imposed strain range. The simulation results obtained using a model with a kinematic hardening without thresholds and those obtained using the present model were compared with experimental tests. The comparison showed that the use of 4 kinematic hardening rules with thresholds is necessary to accurately describe the mean stress relaxation [1].

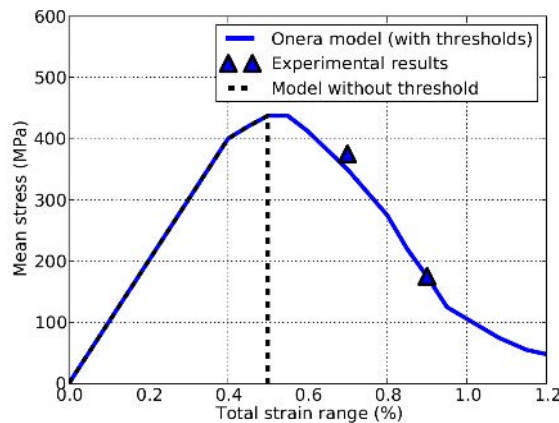


Figure 3: Stabilized mean-stress as a function of the imposed strain range [1].

Numerical procedure. The influence of residual stresses on the lifetime has been characterized on cylindrical specimens machined with the same protocol as the turbine disks. The numerical analysis was performed on a rectangular section of the specimen, meshed with linear triangular axisymmetric elements as shown on Figure 4. In order to introduce and to calculate the evolution of the residual stress profile a progressive mesh is proposed with very small elements close to the surface (~0.04mm) and larger in the center (~0.65mm).

Compared to a standard FE analysis, the proposed one needs a preliminary step which consists in computing the initial mechanical state induced by the residual stresses. It is then necessary to introduce at the very beginning of the calculation not only the plastic strains but all the internal variables in coherence with the initial stress state.

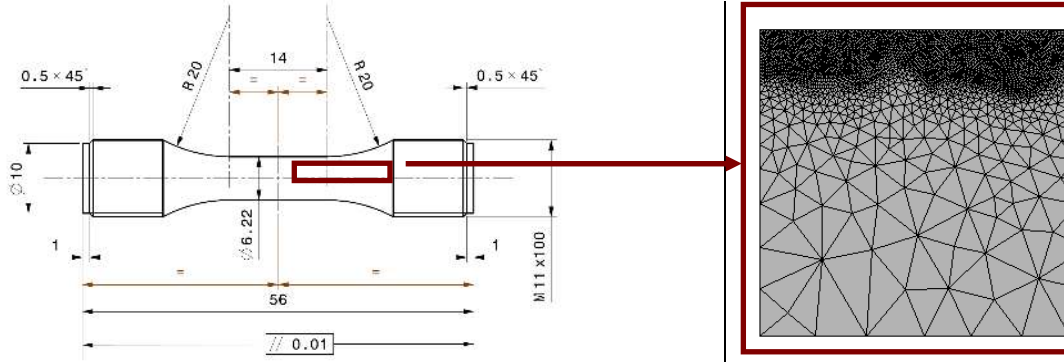


Figure 4: Geometry and meshing of cylindrical fatigue specimen.

The modeling is performed as follows:

- Step 1: The measured residual stress depth profile is fitted by a pseudo-Voigt function (Figure 5). The same profile was taken for hoop and axial stress as a first approximation although they are expected to be slightly different due to equilibrium conditions.
- Step 2: For a set of points of this profile, a FE calculation is performed on a Reference Volume Element (RVE) loaded bi-axially with the measured residual stress values. This calculation is performed to obtain all the internal variables and all the components of the plastic strain tensor. Figure 5 shows, for example, the plastic strain ϵ_{11}^p fitted from the calculation on the RVE.
- Step 3: These internal variables are introduced as initial values in the inelastic cyclic analysis of the specimen in the finite element code Z-set/Zebulon with a special procedure developed for this purpose.
- Step 4: A cyclic calculation is performed using the specific constitutive equations presented above until the stabilized cycle, which is reached after a low number of cycles for these strain load amplitudes.
- Step 5: Finally, starting from the stabilized stress state reached on each integration point of the structure, a post-processing analysis was performed to compute the fatigue life. For this purpose a multiaxial extension of the Smith-Watson-Topper (SWT) [9] model was developed which is able to take into account the strong influence of the mean-stress on the lifetime. The model is summarized as follows:

$$\Gamma = \sqrt{E \sigma_{aeq} \epsilon_{aeq} \left(1 + \frac{(Tr \sigma)_{mean}}{\sigma_{aeq}} \right)} = B N_f^{-\beta} + A N_f^{-\alpha}$$

$$\text{with } \sigma_{aeq} = \text{Max}_{t_0} \text{Max}_t \sqrt{\frac{3}{2} (\underline{\sigma}'(t) - \underline{\sigma}'(t_0)) : (\underline{\sigma}'(t) - \underline{\sigma}'(t_0))},$$

$$\varepsilon_{aeq} = \varepsilon_{aeq}^P + \varepsilon_{aeq}^e = \varepsilon_{aeq}^P + \frac{\sigma_{aeq}}{E} \text{ and } \varepsilon_{aeq}^P = \text{Max}_{t_0} \text{Max}_t \sqrt{\frac{2}{3} (\underline{\varepsilon}^P(t) - \underline{\varepsilon}^P(t_0)) : (\underline{\varepsilon}^P(t) - \underline{\varepsilon}^P(t_0))}$$

where Γ is the SWT parameter, E the Young's modulus and A, B, α and β are the material parameters of the model.

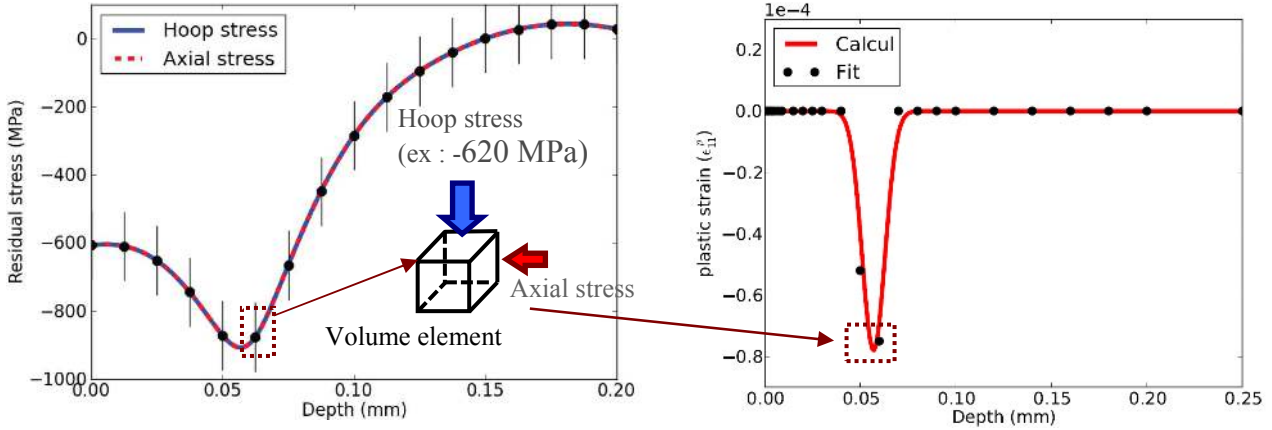


Figure 5: Left: Initial residual stress profile fitted from the profile obtained using X-ray diffraction (Figure 2) - Right: Plastic strain ε_{11}^p fitted from the calculation points.

The obtained fatigue life is then compared to fatigue tests performed at 450°C with $R_\varepsilon=0$ on cylindrical specimens (TGmP and TGmP + shot-peened) for different strain ranges (0.6%, 0.4% and 0.35%).

Results and discussion

The finite element simulation was performed at controlled total strains with three strain ranges ($\Delta\varepsilon/2 = 0.35\%$, $\Delta\varepsilon/2=0.4\%$ and $\Delta\varepsilon/2 =0.6\%$) for $R_\varepsilon=0$. The stabilized cycle is reached after about 100 cycles. Figure 6 shows the imposed strain ranges as a function of the fatigue life. The results of the present calculations (red dotted line), which take into account residual stresses are compared with the calculations of Boittin [1], which do not include RS. Fatigue test results are superimposed: blue squares for the TGmP specimens and red triangles for shot-peened TGmP specimens.

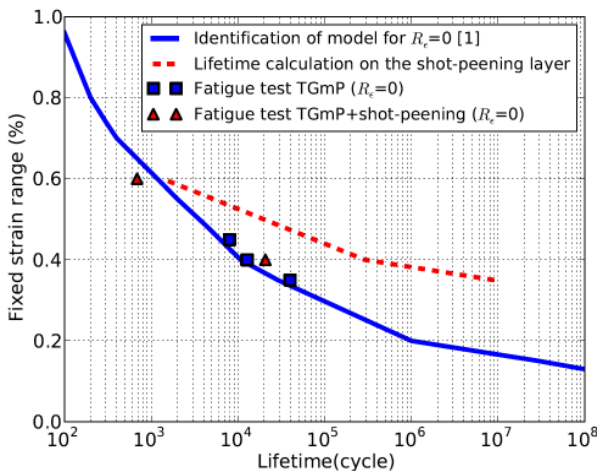


Figure 6: Imposed strain range versus fatigue life (cycle).

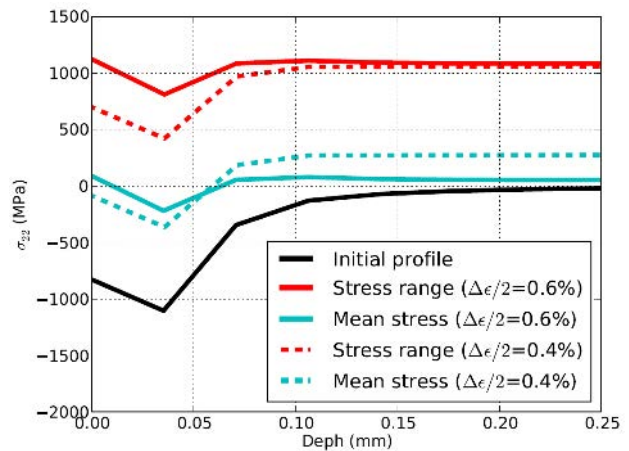


Figure 7: Comparison between initial residual stress profile and stress range and mean stress at the stabilized cycle (for $\Delta\varepsilon/2 = 0.4\%$ and $\Delta\varepsilon/2=0.6\%$).

In this figure, it can be observed that, according to the model, residual stresses associated with shot-peening increase significantly the lifetime of the outer layer. This benefit is higher when the strain amplitude is low. However, above 0.6%, shot-peening has no effect probably due to a faster relaxation of the stresses. Indeed Figure 7 shows that for $\Delta\varepsilon/2=0.6\%$ the stress range and the mean stress at the surface at the stabilized cycle are close to those at the subsurface unlike the case of $\Delta\varepsilon/2=0.4\%$. This behavior is not clearly observed in the measurements since the lifetime of the TGmP and shot-peened TGmP specimens are very close for all the tested strain ranges. This can be explained by the fact that, under fatigue conditions (traction-compression testing), the whole cross-section of the specimen is homogeneously loaded, with no mechanical gradients unlike to bending tests for instance. The benefit of compressive stresses at the surface is counterbalanced by a tensile residual stress in the subsurface area and thus the lifetime of the two specimens should not be so different. Additional Scanning Electron Microscopy (SEM) studies show that for the shot-peened TGmP specimen at $\Delta\varepsilon/2=0.4\%$ the crack nucleation site is located at 1 mm beneath the surface (Figure 8) whereas it is located at the surface for the TGmP specimen (Figure 9). Moreover a multiple cleavage is observed for the shot-peened specimen corresponding to $\Delta\varepsilon/2=0.6\%$. These results tends to show that shot-peening tends to move the crack nucleation sites deeper into the material and could then have an impact on lifetime in fatigue conditions (traction-compression testing).

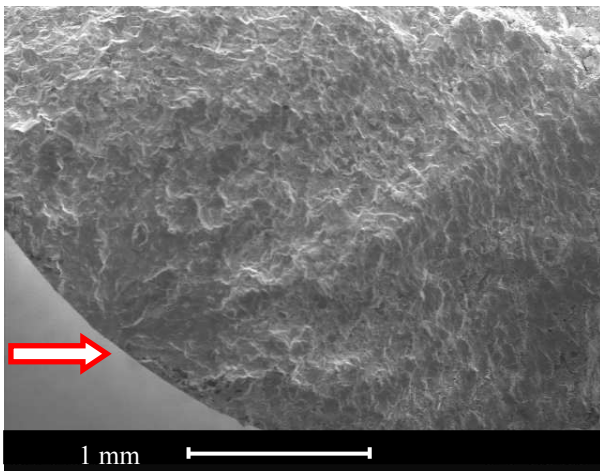


Figure 8: Fatigue fracture surface of TGmP fatigue specimen at $\Delta\varepsilon/2 = 0.4\%$.

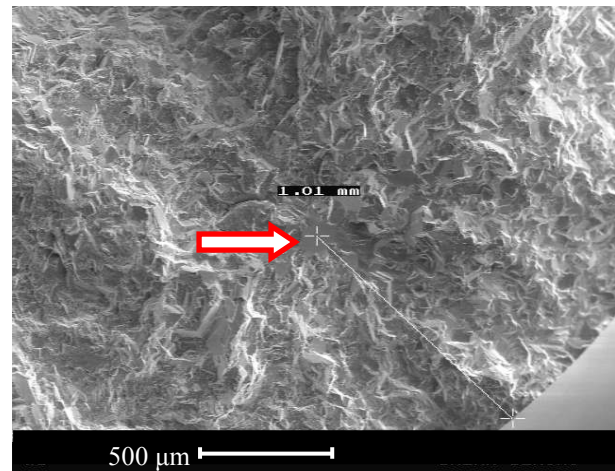


Figure 9: Fatigue fracture surface of TGmP+shot-peened specimen at $\Delta\varepsilon/2 = 0.4\%$.

Conclusion and future work

The aim of this study was to determine some residual stress levels associated to shot-peening on a representative turbine disc specimen made of the N18 superalloy using the $\sin^2 \Psi$ method and to assess experimentally and numerically the influence of residual stresses on the lifetime associated to cyclic fatigue conditions at 450°C.

The residual stress measurements on shot-peened specimen using a high resolution diffractometer provided satisfactory results for the affected zone. However grain size issues are reached beneath 80 μm , which make the $\sin^2 \Psi$ method unsuitable. The benefits of a further increase in the beam size, the beam divergence or the amplitude of oscillation would be limited. A single crystal method applied to individual grains, albeit time consuming, may be more suitable.

Finite element calculations were performed allowing to take into account residual stress profiles and their relaxation to determine the lifetime of the surface layer of N18 shot-peened samples during cyclic loading at 450°C. The results from the model demonstrate that a pre-stressing treatment is beneficial only for small strain ranges. However, the fatigue tests tend to show that crack nucleation is moved deeper into to material for shot-peened samples whereas it is located at the surface for other samples.

Future work will concern the improvement of the X-ray method used to determine the residual stress profiles of such superalloy and additional fatigue tests will be undertaken in order to assess the trends suggested by the calculations.

References

- [1] G. Boittin, Expérimentation numérique pour l'aide à la spécification de la microstructure et des propriétés mécaniques d'un superalliage base Ni pour des applications moteur, PhD thesis, Mines ParisTech (2011).
- [2] J.-L. Chaboche, O. Jung, Application of a kinematic hardening viscoplasticity model with thresholds to the residual stress relaxation, *Int. J. Plasticity* 13 (1998) 785-807.
- [3] M.A.S. Torres, H.J.C. Voorwald, An evaluation of shot peening, residual stress and stress relaxation on fatigue life of AISI 4340 steel, *Int. J. Fatigue* 24 (2002) 877-886.
- [4] K. Dalaei, B. Karlsson, L.-E. Svensson, Stability of shot peening induced residual stresses and their influence on fatigue lifetime, *Materials Science and Engineering A* 528 (2011) 1008-1015.
- [5] V. Hauk, *Structural and Residual Stress Analysis by Non-destructive Methods* (1997) Elsevier Science B.V. ISBN 978-0-444-82476-9.
- [6] AFNOR, *Non-destructive testing – Test methods for measurement of residual stress analysis by X-ray diffraction*, CEN/TC 138 N666, (2004).
- [7] S. Wang, Y. Li, R. Wang, Compressive residual stress introduced by shot peening, *Journal of Materials Processing Technology* 73 (1998) 64-73.
- [8] J.-L. Chaboche, P. Kanouté, F. Azzouz, Cyclic inelastic constitutive equations and their impact on the fatigue life prediction, *Int. J. Plasticity* 35 (2012) 44-66.
- [9] V. Bonnard, J.L. Chaboche, P. Gomez, P. Kanouté, D. Pacou, Investigation of multiaxial fatigue in the context of turboengine disc applications, *Int. J. Fatigue* 33 (2011) 1006-1016.